A modification to the van Genuchten model for improved prediction of relative hydraulic conductivity of unsaturated soils

Xingxing Kuang[1,2*], Jiu Jimmy Jiao[3,4], Jipeng Shan[1], Zhenlei Yang[5]

[1] State Environmental Protection Key Laboratory of Integrated Surface Water-Groundwater Pollution Control, School of Environmental Science and Engineering, Southern University of Science and Technology, Shenzhen 518055, China

[2] Shenzhen Municipal Engineering Lab of Environmental IoT Technologies, Southern University of Science and Technology, Shenzhen 518055, China

[3] Department of Earth Sciences, The University of Hong Kong, Pokfulam Road, Hong Kong, China

[4] The University of Hong Kong, Shenzhen Research Institute (SRI), Shenzhen, China

[5] Institute of Bio- and Geosciences: Agrosphere (IBG3), Forschungszentrum Jülich GmbH, 52425 Jülich, Germany

***Corresponding author:** Xingxing Kuang, E-mail: kuangxx@sustech.edu.cn

Running title: Modified van Genuchten model

This article has been accepted for publication and undergone full peer review but has not been through the copyediting, typesetting, pagination and proofreading process which may lead to differences between this version and the Version of Record. Please cite this article as doi: 10.1111/ejss.13034

Abstract

Modeling of flow and transport in unsaturated soils requires information on two fundamental hydraulic properties: soil water retention curve and relative hydraulic conductivity. A soil's relative hydraulic conductivity is frequently predicted from soil water retention curve. The most widely used combination is the van Genucthen model for soil water retention curve and the Mualem model for relative hydraulic conductivity (VGM). Previous studies show that the VGM model underestimates measured relative hydraulic conductivity for soils with fine-textures, a sharp drop in relative hydraulic conductivity can be seen near saturation. A new modification of the van Genuchten soil water retention model is proposed with the aim of improving the agreement between predicted and measured relative hydraulic conductivity. The Brooks and Corey-Burdine model is used to predict relative hydraulic conductivity from the modified van Genuchten soil water retention curve (MVG-BCB). The modified model assumes independent m and n in the van Genuchten model but with constraints $n > 2$ and $0 < m < 1$. The MVG-BCB model is evaluated by comparing calculated and measured data for 59 soils that have widely varying soil textures, ranging from sandstone to clay. The MVG-BCB model improves the agreement between calculated and measured data for both soil water retention curve and relative hydraulic conductivity. The MVG-BCB model is closer to measured relative hydraulic conductivity data for most of the select soils and the sharp drop near saturation is eliminated. Both the modified soil water retention curve and relative hydraulic conductivity functions are smooth curves and can easily be incorporated into vadose zone flow and transport modellings.

Keywords: soil water retention curve, relative hydraulic conductivity, soil hydraulic properties, van Genuchten model, infiltration

Highlights

A new modification to the van Genuchten soil water retention model

The model improves the fit to measured soil water retention data

The chosen model improves the prediction of relative hydraulic conductivity

1. INTRODUCTION

Soil water retention curve and relative hydraulic conductivity are the two basic hydraulic properties of unsaturated soils. These unsaturated hydraulic properties are needed in numerical modeling of water flow (e.g., infiltration, evaporation, and drainage) and solute transport in soils. The van Genuchten (1980) model is the most widely used model for soil water retention curve and the van Genuchten-Mualem (VGM) model (Mualem, 1976; van Genuchten, 1980) has been the most frequently used model for relative hydraulic conductivity. The van Genuchten (1980) soil water retention curve is smooth and the derived relative hydraulic conductivity function such as the VGM model has a closed-form expression. However, a sharp drop in relative hydraulic conductivity can be observed near saturation for fine textured soils (Iden et al., 2015; Ippisch et al., 2006; Touma, 2009; van Genuchten & Nielsen, 1985; Vogel et al., 2001), hence the relative hydraulic conductivity is significantly underestimated. The constraints on the parameters of the VGM model (m and n) have been analyzed by several previous studies (Fuentes et al., 1992; Ippisch et al., 2006; Luckner et al., 1989).

Many researchers attempted to improve the performance of the VGM model. Van Genuchten and Nielsen (1985) assumed the parameters m and n in the van Genuchten (1980) model are mutually independent and derived the general VGM model for relative hydraulic conductivity. Although assuming variable m and n leads to improved fit to soil water retention curve, the sharp drop in relative hydraulic conductivity near saturation is not eliminated when n approaches 1. Vogel and

Cislerova (1988) replaced the saturated water content θ_s in the van Genuchten (1980) model by a fitting parameter θ_m ($\theta_m \geq \theta_s$), as a result, both the soil water retention curve and the relative hydraulic conductivity are composed of two parts: a linear part ($0 \leq h \leq h(\theta_s)$) and a nonlinear part ($h > h(\theta_s)$). Schaap and Leij (2000) pointed out that the pore tortuosity and pore connectivity parameter in the relative hydraulic conductivity equation is predominantly negative. Such a modification only applicable to situations away from saturation and a underestimation of relative hydraulic conductivity probably happen near saturation (Schaap & Leij, 2000). Iden et al. (2015) introduced a maximum pore radius in the Mualem (1976) capillary bundle model and derived an expression for relative hydraulic conductivity. Although there is improvement for the predicted relative hydraulic conductivity, the sharp drop in relative hydraulic conductivity can still be seen near saturation when $n < 2$. Troch (1993) assumed $m = 1 + 1/n_1$ ($n_1 \neq n$) in the van Genuchten (1980) soil water retention curve. Based on the work of Troch (1993), Kong et al (2016) and Luo et al. (2019) proposed a similar expression for relative hydraulic conductivity but with $m = 1 + 1/n_2$ ($n_2 \neq n_1$). Two additional parameters are required for such modifications and Luo et al. (2019) proposed a complicated empirical polynomial expression for calculating n_2 from n_1. Furthermore, the soil water retention curve may be underestimated when saturation is relatively low.

Researchers also attempted to improve the VGM model by introducing an air entry value in the van Genuchten (1980) soil water retention curve function. Vogel et al. (2001) proposed a very small minimum capillary height h_s in the van Genuchten (1980) function. Vogel et al. (2001) pointed out that the minimum capillary height h_s will lead to less nonlinearity in relative hydraulic conductivity near saturation, but only one soil was used. On the basis of Vogel et al. (2001), Schaap and van Genuchten (2006) introduced a small air entry pressure h_s in the van Genuchten (1980) function and linear correction was used for relative hydraulic conductivity near saturation. The air entry pressure h_s was set to be a constant as $h_s = -4$ cm and piece-wise linear expressions have to be used to correct predicted relative hydraulic conductivity. Kuang and Jiao (2014) introduced an air entry value h_a in the soil water retention curve based on the van Genuchten (1980) function. The air entry value h_a vary with different soils but the soil water retention curve and relative hydraulic conductivity may not be smooth near h_a when *n* approaches 1.

Power law relative hydraulic conductivity models have long been established. Many researchers presented the general form of the power law relative hydraulic conductivity function (e.g., Assouline, 2001, 2005; Assouline & Or, 2013; Brutseart, 1967, 2000; Hayek, 2016; Mualem, 1976, 1978). Early studies considered the power value to be a constant that ranges from 2.0 to 7.2 (Averjanov, 1950; Bresler et al., 1978; Irmay, 1954; Yuster, 1951). Mualem (1978) generalized the power law relative hydraulic conductivity model by allowing the power value to change with soil type and found that the power value varies between 2.5 and 24.5. Substituting the Brooks and Corey (1964) soil water retention curve into the generalized capillary bundle model (Assouline & Or, 2013; Assouline & Selker, 2017; Hayek, 2016; Kosugi, 1999; Mualem & Dagan, 1978) leads to the generalized power law relative hydraulic conductivity function (e.g., Hayek, 2016; Madi et al., 2018). Different expressions have been proposed for the relationship between the power and the pore size distribution index of the Brooks and Corey (1964) model based on experimental datasets (Assouline, 2005; Brutsaert, 2000).

The power law relative hydraulic conductivity models have been verified to provide satisfactory predictions of measured data (Fuentes et al., 1992; Kuang & Jiao, 2014; Mualem, 1978; Touma, 2009). Fuentes et al. (1992) pointed out that the best combination is the van Genuchten (1980) soil water retention curve with the Burdine (1953) constraint $m = 1 - 2/n$ and the Brooks and Corey (1964)-Burdine (1953) function for relative hydraulic conductivity. Kuang and Jiao (2014) also found that the use of Brooks and Corey (1964)-Burdine (1953) function for relative hydraulic conductivity gives satisfactory match to measured data. Touma (2009) found that the most reliable combination is the van Genuchten (1980) soil water retention curve with the Fatt and Dykstra (1951) constraint $m = 1 - 2.5/n$ and the Brooks and Corey (1964)-Fatt and Dykstra (1951) function for relative hydraulic conductivity.

The aims of this paper are to 1) propose new constraints on the parameters m and n in the van Genucthen (1980) model and evaluate the modified retention model with experimental data collected from the literature and 2) evaluate the capability of the combination of the modified van Genucthen (1980) model and the Brooks and Corey (1964)-Burdine (1953) model to predict relative hydraulic conductivity. We assumed that the fit to measured soil water retention curve and the prediction of relative hydraulic conductivity are improved by the MVG-BCB model. The resulting modified van Genuchten (1980) model and relative hydraulic conductivity model are continuous smooth curves and the sharp drop of relative hydraulic conductivity near saturation is eliminated. In addition, no new parameter is introduced into both the soil water retention curve and relative hydraulic conductivity model. The combination of the modified van Genucthen (1980) model and the Brooks and Corey (1964)-Burdine (1953) model are easy to use in flow and transport studies.

2. THEORY

2.1 Proposed model

The soil water retention curve is described by the van Genuchten (1980) model

$$\theta(h)=\theta_r+(\theta_s-\theta_r)[1+(\alpha h)^n]^{-m} \quad (n>2\,,\ 0<m<1) \tag{1}$$

where θ is the volumetric water content, θ_s is the saturated volumetric water content, θ_r is the residual volumetric water content, h is the pressure head, α, n, and m are fitting parameters. The pressure head h in Equation (1) is assumed to be positive in order to simplify notation (van Genuchten, 1980). Unlike the original van Genuchten (1980) model, here parameters m and n were assumed to be independent in Equation (1) but with constraints $n>2$ and $0<m<1$. The constraint on n was set based on previous studies (Fuentes et al., 1992; Iden et al., 2015; Ippisch et al., 2006; Luckner et al., 1989). The constraint on m was from the original van Genuchten (1980) model.

The Brooks and Corey (1964)-Burdine (1953) model was chosen to calculate relative hydraulic conductivity (van Genuchten, 1980)

$$K_r(\theta)=S_e^{3+\frac{2}{mn}}=\left(\frac{\theta-\theta_r}{\theta_s-\theta_r}\right)^{3+\frac{2}{mn}} \tag{2}$$

where K_r is the relative hydraulic conductivity and S_e is the effective water saturation defined as $S_e=(\theta-\theta_r)/(\theta_s-\theta_r)$. Equation (2) can provide satisfactory prediction of measured relative hydraulic conductivity data (Fuentes et al., 1992; Kuang & Jiao, 2014). The combination of Equation (1) with $n>2$ and $0<m<1$ and Equation (2) is referred to as the modified van Genuchten (1980)-Brooks and Corey (1964)-Burdine (1953) model (MVG-BCB). The corresponding relative hydraulic conductivity can also be written as

$$K_r(h) = \frac{1}{[1+(\alpha h)^n]^{3m+\frac{2}{n}}} \tag{3}$$

2.2 Models for comparison

Solving Equation (1) for $h(S_e)$ and substituting it into the Mualem (1976) relative permeability model lead to (van Genuchten, 1980)

$$K_r(\theta) = S_e^{1/2}\left[1-(1-S_e^{1/m})^m\right]^2 \tag{4}$$

Equation (1) with $m = 1-1/n$ and Equation (4) are referred to as the VGM model (Mualem, 1976; van Genuchten, 1980). The VGM model is the most widely used model for predicting K_r from the soil water retention curve $\theta(h)$. The corresponding relative hydraulic conductivity $K_r(h)$ can be written as (van Genuchten, 1980)

$$K_r(h) = [1+(\alpha h)^n]^{-m/2}\left\{1-(\alpha h)^{n-1}[1+(\alpha h)^n]^{-m}\right\}^2 \tag{5}$$

The use of Equation (1) with $m = 1-2/n$ to fit the soil water retention curve and Equation (2) to predict relative hydraulic conductivity is referred to as the VG-BCB model (Burdine, 1953; Brooks & Corey, 1964; van Genuchten, 1980). The corresponding relative hydraulic conductivity $K_r(h)$ is also calculated by Equation (3). The VG-BCB model has also been pointed out by previous researchers that it is the best combination for power law relative hydraulic conductivity functions (Fuentes et al., 1992).

The models described here are only applicable for rigid soils. Their volume will not change during wetting and drying. For non-rigid soils, there will be changes in volume during the wetting and drying processes. Previous studies have shown that the expansion and contraction of soils will have a significant impact on the soil water retention curve (e.g., Romero et al., 2011; Chen et al., 2020). Many models have also been proposed to describe the soil water retention curve and relative hydraulic conductivity for deformable soils (e.g., Chen et al., 2020; Hu et al., 2013; Huang et al., 1998; Tao et al., 2019). However, further investigations of the models for soil water retention curve and relative hydraulic conductivity of deformable soils are beyond the scope of this study.

3. MATERIALS AND METHODS

Experimental soil water retention and relative hydraulic conductivity data were collected from the literature to compare the performances of the different models. The methods have been used in previous studies to measure the soil water retention curve including column drainage (Childs & Collis-George, 1950; Dury et al., 1998; Jackson et al., 1965; Kastanek, 1971; Poulovassilis, 1970a, 1970b; Topp, 1971), column infiltration (Haverkamp et al., 1977; Touma & Vauclin, 1986), liquid permeameter and multiple flow cell (Brooks & Corey, 1964), pressure membrane (Elrick & Bowman, 1964), pressure plate and millipore filters (Green et al., 1964), and multistep outflow method (Tuli & Hopmans, 2004). Different methods have also been applied to measure the soil water retention curve of a soil in different pressure ranges, including vapor pressure data, Richards' pressure plate and pressure membrane, and Haines-type apparatus (Staple, 1965). The volumetric water content was measured by indirect electrical methods (Childs & Collis-George, 1950), gamma ray attenuation (Haverkamp et al., 1977; Jensen & Hanks, 1967; Topp, 1971; Touma & Vauclin, 1986; Watson, 1967), and mass balance method (Dury et al., 1998; Poulovassilis, 1970a, 1970b). The pressure head was measured by tensiometers (Black et al., 1969; Haverkamp et al., 1977; Jensen & Hanks, 1967; Kastanek, 1971; Poulovassilis, 1970a, 1970b; Topp, 1971; Touma & Vauclin, 1986; Watson, 1967) and Tempe pressure cells (Tuli & Hopmans, 2004).

A total of 59 soils were selected, 37 of them were selected from the literature and 22 of them were chosen form the UNSODA database (Leij et al., 1996; Nemes et al., 1999; Nemes et al., 2001). The 37 soils are nearly all the soils with measured soil water retention curve and relative hydraulic conductivity data which are available from the literature. The 22 soils from UNSODA are with more than 10 or nearly 10 data points for both soil water retention curve and relative hydraulic conductivity. In addition, the measured $\theta(h)$ and $K_r(h)$ or $K_r(\theta)$ data are smooth for the 22 soils. The 22 soils were selected more or less arbitrarily and it seems adequate for a demonstration purpose. The soils represent widely varying soil textures ranging from sandstone to clay (Table 1). Also shown in Table 1 are the measured saturated hydraulic conductivity K_s and saturated volumetric water content θ_s of the soils.

Equation (1) was fitted to the measured data for every soil with constraints of $m = 1 - 1/n$, $m = 1 - 2/n$, and m and n being independent with $n > 2$ and $0 < m < 1$, respectively. The VGM model and the VG-BCB model were used as reference models. The nonlinear least squares method of Levenberg-Marquardt (Marquardt, 1963; Press et al., 1992) was used to fit the soil water retention curves to the measured data. For the van Genuchten model with $m = 1 - 1/n$ and $m = 1 - 2/n$, the objective function F for parameter estimation can be written as

$$F = \min \sum_{i=1}^{N} \left[\theta_i - \theta(h_i, \theta_r, \alpha, n)\right]^2 \tag{6}$$

For the van Genuchten model with the proposed constraints, the objective function for parameter estimation can be written as

$$F = \min \sum_{i=1}^{N} \left[\theta_i - \theta(h_i, \theta_r, \alpha, n, m)\right]^2 \tag{7}$$

The fitted parameters for different models are listed in Table 2. Only the soil water retention data were fitted and relative hydraulic conductivity was predicted using the

VGM model, the VG-BCB model, and the MVG-BCB model, respectively, using the fitted parameters.

For each soil, the root-mean-square-error (RMSE) was applied to evaluate the fit to the measured soil water retention data

$$\mathrm{RMSE} = \sqrt{\frac{1}{N}\sum_{i=1}^{N}\left[\theta_i - \theta(h_i)\right]^2} \quad (8)$$

where N is the number of measured data points, θ_i and $\theta(h_i)$ are the measured and calculated volumetric water contents. The RMSE was also used to compare the measured and calculated relative hydraulic conductivity data

$$\mathrm{RMSE} = \sqrt{\frac{1}{N}\sum_{i=1}^{N}\left[K_{ri} - K_r(\eta_i)\right]^2} \quad (9)$$

where K_{ri} is the measured relative hydraulic conductivity of the soil, $K_r(\eta_i)$ is the calculated relative hydraulic conductivity by the VGM model, the VG-BCB model, or the MVG-BCB model, and η_i represents either h_i or θ_i.

In addition to RMSE, the coefficient of determination R^2 was also applied to show the goodness of fit. The coefficient of determination R^2 for soil water retention can be written as (Mendenhall & Sincich, 2012)

$$R^2 = 1 - \frac{\sum_{i=1}^{N}[\theta_i - \theta(h_i)]^2}{\sum_{i=1}^{N}(\theta_i - \overline{\theta})^2} \quad (10)$$

where $\overline{\theta}$ is the mean of the measured volumetric water content. R^2 for relative hydraulic conductivity K_r can be expressed as

$$R^2 = 1 - \frac{\sum_{i=1}^{N}[K_{ri} - K_r(\eta_i)]^2}{\sum_{i=1}^{N}(K_{ri} - \bar{K}_r)^2} \tag{11}$$

where $\bar{K}_r$ is the mean of the measured relative hydraulic conductivity.

4. RESULTS

4.1 Illustrative examples

A comparison between measured and calculated soil water retention curve and relative hydraulic conductivity for four soils are presented in Figure 1. The relative hydraulic conductivity is expressed as $K_r(\theta)$. The four examples represent four types of soils, i.e., sand, loam, silt clay loam, and clay. The shapes of the measured soil water retention curves of the four soils are quite different from each other. In addition, the four examples clearly exhibits the improvement of the MVG-BCB model.

For Mixed sand (Dury et al., 1998), all the models provide a good fit to the measured soil water retention curve. The RMSE of the MVG-BCB model is slightly smaller than others and the R^2 of the MVG-BCB model is the greatest. All the relative hydraulic conductivity models provide very good prediction of the measured data. Although the MVG-BCB model yields the smallest RMSE and the greatest R^2 values, the MVG-BCB model and the VG-BCB model are very similar to each other. The curves calculated by the two models are nearly indistinguishable. For this soil, the VGM model also agrees with the measured data very well.

For soils with soil water retention curve similar to the Mixed sand, the fitted n will be greater than 2 in the original van Genuchten (1980) model. The fitted n in the original van Genuchten model for the Mixed sand is $n = 5.773$, as shown in Table 2. For such soils, the VGM model can produce good prediction of the relative hydraulic conductivity. There will be no sharp drop in relative hydraulic conductivity near saturation for the VGM model. Improvement by the MVG-BCB model or the VG-BCB model may not be significant.

For Guelph loam (Elrick & Bowman, 1964) and Yolo light clay (Haverkamp et al., 1977; Philip, 1957), the agreement between measured and calculated soil water retention curve data for different models are similar to each other. The RMSE of the MVG-BCB model is the smallest, slightly smaller than that of the VG-BCB model. The MVG-BCB model can present a quite good fit to the measured soil water retention curve. The residual volumetric water content θ_r fitted by the MVG-BCB model is smaller than that of the other models. The RMSE value of the MVG-BCB model is also the smallest and the R^2 value is the greatest for relative hydraulic conductivity. The MVG-BCB model provides very good predictions of the measured relative hydraulic conductivity data for these two soils. Furthermore, the MVG-BCB model and the VG-BCB model also give very similar results. The two curves are also nearly indistinguishable from each other.

The Guelph loam and Yolo light clay are two soils with n values in the original van Genuchten model small than 2 (Table 2). Improvements in both $\theta(h)$ and $K_r(\theta)$ can be seen when using the MVB-BCB model. The sharp drop in relative hydraulic conductivity near saturation was eliminated. The curves calculated by both the MVG-BCB model and the VG-BCB model are very close to the measured relative hydraulic conductivity data. As a result, for soils with $n < 2$ in the original van Genucthen model, the MVG-BCB model can be applied to improve the prediction of relative hydraulic conductivity.

The first three soils (Mixed sand, Geulph loam, and Yolo light clay) show that the performance of the MVG-BCB model is very similar to the VG-BCB model. Although there is one more parameter in the MVG-BCB model when fitting the soil water retention curve than the VG-BCB model, the curve calculated by the VG-BCB model is very close to that of the MVG-BCB model. The corresponding two relative hydraulic conductivity curves are also almost indistinguishable from each other. For soils with measured soil water retention curve similar to those of the three soils, the VG-BCB model is also a good choice, which was already pointed out by previous studies (Fuentes et al., 1992; Kuang & Jiao, 2014). The results of this study support the conclusion that the VG-BCB model is capable of providing good prediction of $K_r(\theta)$ for such soils.

For Weld silty clay loam (Jensen & Hanks, 1967), the agreement between measured and calculated soil water retention data of the MVG-BCB model is also very good and the RMSE value is the smallest and the R^2 value is the greatest. The fit to measured soil water retention data near saturation was improved by the MVG-BCB model. In addition, the MVG-BCB model is also the closest to the measured soil water retention data when the pressure head h is greater than about 100 cm. The θ_r fitted by the MVG-BCB model is smaller than that of the other models. The θ_r value fitted by the VG-BCB model and the VGM model are nearly the same. The improvement of the fit to soil water retention data by the MVG-BCB model is due to one more fitting parameter in the MVG-BCB model. Overall, the curves calculated by the MVG-BCB model, the VG-BCB model, and the VGM model are very close to each other when $K_r(\theta)$ is greater than about 0.1. However, the curve given by the MVG-BCB model is closer to the measured data when $K_r(\theta)$ is smaller than about 0.1. The R^2 value of the MVG-BCB model for $K_r(\theta)$ is also the greatest among these models.

The soil Weld silty clay loam shows that the MVG-BCB model improves the fit to both measured soil water retention data and relative hydraulic conductivity. Due to the fact that the MVG-BCB model is in the best agreement between calculated and measured soil water retention data in relatively high pressure head (i.e., greater than 100 cm), the $K_r(\theta)$ given by the MVG-BCB model is also in the best agreement between measured and calculated relative hydraulic conductivity data when θ is relatively low. A smaller θ_r fitted by the MVG-BCB model leads to improved prediction of relative hydraulic conductivity. For this case, both the VG-BCB model and the VGM model do not fit the measured soil water retention data and relative hydraulic conductivity very well. As a result, for soils with measured soil water retention curve similar to that of the Weld silty clay loam, the MVG-BCB model may be applied to predict $K_r(\theta)$ to improve the agreement between predicted and measured data.

A comparison between calculated and measured soil water retention curve and relative hydraulic conductivity for another four soils are given in Figure 2. The relative hydraulic conductivity is expressed as $K_r(h)$. The fitted parameters for different models of the four soils are also presented in Table 2. The four examples also represent four different types of soils, namely sandstone, sand, silt loam, and sandy loam. The results of these four soils clearly show the improvement of the MVG-BCB model for $K_r(h)$, both near saturation and when pressure head h is relatively high.

For these soils, the RMSE of the MVG-BCB model is the smallest among the three models for soil water retention curve. The MVG-BCB model matches the measured soil water retention data very well. The MVG-BCB model is also the closest to the measured data near saturation. The θ_r fitted by the MVG-BCB model is smaller than the other models for the four soils. Both the VGM model and the VG-BCB model also provide fairly good descriptions of the measured soil water retention data. The soil water retention curves calculated by the VGM model and the VG-BCB model are very close to each other. The R^2 values shown in Figure 2 also support that the MVG-BCB model provides improved description of the measured soil water retention data.

For $K_r(h)$, the MVG-BCB model has the smallest RMSE value for each of the soil. The agreement between predicted and measured $K_r(h)$ near saturation is improved by the MVG-BCB model. The underestimation of measured relative hydraulic conductivity near saturation is also improved by the MVG-BCB model. For Sandy loam (2422), the MVG-BCB model is also closer to the measured data when K_r is relatively low (i.e., $K_r < 0.01$). For the four soils, the VGM model and the VG-BCB model perform similar to each other. For relative hydraulic conductivity near saturation, the VG-BCB model does not eliminate the underestimation of measured relative hydraulic conductivity, though improvements can be seen for Poudre river sand and Silt loam (2231). Compared with the improvement given by the

VG-BCB model for $K_r(\theta)$, the improvement given by the VG-BCB model for $K_r(h)$ is not so significant.

4.2 Statistical analysis

Overall, the introduced constraints on m and n in the van Genuchten (1980) model improved the fit to the measured soil water retention data (Figure 3). Among the 59 soils, the MVG-BCB model has the smallest RMSE value for 44 soils. For many soils, the RMSE value of the MVG-BCB model is significantly smaller than that of the other two models. This is probably due to that one more fitting parameter is added to Equation (1), increasing the degree of freedom and thus flexibility of the equation. The VGM model also has the smallest RMSE value for 12 soils. The RMSE values of the VGM model and those of the VG-BCB model are very similar to each other for most of the soils. There are also 44 soils have the greatest R^2 values for the MVG-BCB model and 12 soils have the greatest R^2 value for the VGM model (Table 3).

For $K_r(\theta)$, the MVG-BCB model has the smallest RMSE value for 20 out of 45 soils (Figure 4a). The VGM model has the smallest RMSE value for 10 soils and the VG-BCB has the smallest RMSE value for 15 soils. The R^2 values in Table 3 also show that the MVG-BCB model has the greatest R^2 for 20 out of 45 soils. The

RMSE values of the MVG-BCB model and the VG-BCB model are very similar to each other. This is probably due to the fact that both models use Equation (2) to calculate relative hydraulic conductivity, though with different m and n values. Figure 4a shows that there is no significantly high RMSE value of the MVG-BCB model. All the RMSE values for the MVG-BCB model are smaller than about 0.25. The results of the 45 soils show that the MVG-BCB model can provide very good predictions of measured relative hydraulic conductivity data.

For $K_r(h)$, the RMSE value is the smallest and the R^2 value is the greatest for 16 out of 23 soils for the MVG-BCB model (Figure 4b and Table 3). The VGM model has the smallest RMSE and the greatest R^2 for 3 soils and the VG-BCB model has the smallest RMSE and the greatest R^2 for 4 soils. The results show that the MVG-BCB model is also able to provide very good predictions of measured $K_r(h)$ data. There is again no extremely large RMSE value for the MVG-BCB model (Figure 4b). Compared with $K_r(\theta)$, the improvement in $K_r(h)$ by the MVG-BCB model is more evident.

5. APPLICATIONS

Two one-dimensional ponded infiltration experiments were used to further compare the three models. Cumulative infiltration $V(t)$ was calculated for both

Grenoble sand (Parlange et al., 1985) and Yolo light clay (Haverkamp et al., 1977; Haverkamp et al., 1990). The infiltration process was simulated by the saturated-unsaturated flow code OSUNF (Kuang et al., 2011). The cumulative infiltration $V(t)$ at time level j can be calculated as (Kuang et al., 2011)

$$V^j = \sum_{i=1}^{M-1} \left(\frac{\theta_i^j + \theta_{i+1}^j}{2} - \frac{\theta_i^0 + \theta_{i+1}^0}{2} \right) \Delta z \quad (12)$$

where M is the total number of nodes in the model, and θ^j and θ^0 are the volumetric water content at time level j and $t = 0$, respectively.

For Grenoble sand, the soil water retention curve and relative hydraulic conductivity is shown in Figure 5. The saturated hydraulic conductivity K_s and soil water retention curve parameters of the Grenoble sand are given in Tables 1 and 2, respectively. Details on the infiltration experiment can be found in Parlange et al. (1985). The column is 0.935 m long and was discretized into 188 nodes with a uniform $\Delta z = 0.5$ cm. The upper boundary of the column was assigned a constant head boundary of $h_0 = 2.3$ cm. The time step is constant as $\Delta t = 1$ s and the total simulation time is 0.4 h.

For Yolo light clay, the soil water retention curve and relative hydraulic conductivity is presented in Figure 1. The saturated hydraulic conductivity K_s and soil water retention curve parameters are also shown in Tables 1 and 2, respectively. Cumulative infiltration data on Yolo light clay are presented in Haverkamp et al.

(1977) and Haverkamp et al. (1990). The column was set to be 1 m long and was discretized into 1001 nodes with a uniform $\Delta z = 0.1$ cm. The upper boundary of the column was assigned a constant head boundary of $h_0 = 10$ cm. The time step is constant as $\Delta t = 360$ s and the total simulation time is 150 h.

A comparison of the calculated and measured cumulative infiltration is shown in Figure 6. For Grenoble sand, the MVG-BCB model provides a reasonably good prediction of cumulative infiltration. The curves of the VG-BCB model and the MVG-BCB model are nearly indistinguishable between each other, but the MVG-BCB model is slightly closer to the experimental data. The MVG-BCB model performs the best for this case. For Yolo light clay, the MVG-BCB model also agrees with the experimental data very well. The MVG-BCB model and the VG-BCB model are also indistinguishable between each other. Overall, the MVG-BCB model improves the agreement between calculated and measured cumulative infiltration data for the two soils.

6. DISCUSSION

The MVG-BCB model is mathematically simple and easy to use. No new equation was introduced and both the soil water retention curve and relative hydraulic conductivity of the MVG-BCB model are smooth curves. For $K_r(\theta)$, the MVG-BCB model eliminates the sharp drop in relative hydraulic conductivity when n is smaller than 2 in the VGM model. For $K_r(h)$, the MVG-BCB model also improves the agreement between predicted and measured $K_r(h)$ near saturation.

The power law relative hydraulic conductivity is a good choice for predicting $K_r(h)$ or $K_r(\theta)$ from soil water retention curves (Fuentes et al., 1992; Kuang & Jiao, 2014; Touma, 2009). But the MVG-BCB model and the VG-BCB model tend to slightly overestimate relative hydraulic conductivity for some soils. For example, both the MVG-BCB model and the VG-BCB model slightly overestimated measured relative hydraulic conductivity of Grenoble sand (Figure 5). As a result, the cumulative infiltration calculated using the two models slightly overestimated the measured data (Figure 6).

Although the VG-BCB model can significantly improve the prediction of $K_r(\theta)$, it does not significantly improve the prediction of $K_r(h)$. As can be seen from Guelph loam and Yolo light clay in Figure 1, the sharp drop in relative hydraulic conductivity near saturation is eliminated by the VG-BCB model. The curve given by the VG-BCB model is almost indistinguishable from that of the MVG-BCB model. The VG-BCB model also shows improvement in predicted $K_r(h)$, as can also been seen in the R^2 values in Figure 2. The improvement is most significant for Pouder river sand and Silt loam (2231). However, the VG-BCB model still underestimates the measured $K_r(h)$ data near saturation. The underestimation of $K_r(h)$ near saturation is eliminated by the MVG-BCB model.

Although the MVG-BCB model has one more parameter when fitting the soil water retention data, there are still 12 soils have the smallest RMSE and the greatest R^2 values for the VGM model. From soils with number 49-59, the VGM model has the smallest RMSE and the greatest R^2 for 6 out of 11 soils (Figure 3 and Table 3). As can be seen from Table 2, these soils mostly have n values small than 2 in the VGM model. The VGM model performs very good in fitting soil water retention data with n value small than 2. These soils are mainly fine textured soils including silt loam, silty clay loam, silty clay, and clay. However, the performance of the VGM model for $K_r(\theta)$ and $K_r(h)$ are not so good for these soils, which is mainly due to the sharp drop of the VGM model near saturation. A significant underestimate of measured relative hydraulic conductivity is caused by the sharp drop. The sharp drop in relative hydraulic conductivity has been attributed to the capillary model of Mualem (1976), as pointed out by previous studies (Iden et al., 2015; Vogel et al., 2001). The MVG-BCB model performs good on these soils and it has the smallest RMSE and the greatest R^2 for most of the soils, both for $K_r(\theta)$ and $K_r(h)$. As the original and modified van Genuchten functions can fit the measured soil water retention data very well, improved or new capillary models may be developed to improve the prediction of measured relative hydraulic conductivity data.

This study introduced new constraints on the parameters m and n in the van Genuchten (1980) soil water retention curve model. Relative hydraulic conductivity was predicted from the fitted parameters of the soil water retention curve using the VGM model, the VG-BCB model, and the MVG-BCB model, respectively. All parameters in the relative hydraulic conductivity models are obtained from soil water retention curve. The relative hydraulic conductivity equation in the VG-BVB model and the MVG-BCB model is the same, as shown in Equation (2). For the VGM model, Equation (4) was applied to predict relative hydraulic conductivity. In Equation (4), the power $1/2$ may be take as a fitting parameter and it may change with different soil types (Schaap & Leij, 2000). As we focused on predicting $K_r(\theta)$ or $K_r(h)$ from soil water retention curve, the power was fixed at $1/2$ (Mualem, 1976). Researchers pointed out that changing $1/2$ into a fitting parameter can improve the agreement between predicted and measured relative hydraulic conductivity data (Schaap & Leij, 2000).

7. CONCLUSIONS

A MVG-BCB model with improved prediction of $K_r(\theta)$ and $K_r(h)$ was proposed. New constraints on the parameters m and n were introduced into the van Genuchten (1980) model with $n > 2$ and $0 < m < 1$ and the modified model was compared to measured soil water retention data. On the basis of 59 soils that covering a wide range of soil textures, the modified van Genuchten (1980) model can provide improved fit to the measured soil water retention data for most of the selected soils. The fit to measured data both near saturation and in relatively high pressure heads are improved by the MVG-BCB model.

The MVG-BCB model can give improved predictions of measured relative hydraulic conductivity for both $K_r(\theta)$ and $K_r(h)$. The MVG-BCB model eliminates the sharp drop in $K_r(\theta)$ near saturation when n is smaller than 2 in the VGM model. The MVG-BCB model also eliminates the underestimation of measured $K_r(h)$ near saturation. It can provide improved predictions of measured $K_r(h)$ when pressure head h is relatively high. The RMSE values are relatively small for all the 59 soils and the R^2 values are relatively great for the soils. The results show that power law relative hydraulic conductivity models can provide good predictions of measured data.

All the $\theta(h)$, $K_r(h)$, and $K_r(\theta)$ functions are smooth curves for the MVG-BCB model. The MVG-BCB model is also mathematically simple and can be easily incorporated in numerical models on unsaturated flow and solute transport. The MVG-BCB model is able to improve the agreement between calculated and measured cumulative infiltration for both Grenoble sand and Yolo light clay. The constraints on m and n in the modified van Genuchten (1980) model was based on previous studies and can be seen as empirical. The MVG-BCB model seems to be suited for all types of soils, especially for fine-textured soils with n smaller than 2 in the van Genuchten (1980) soil water retention curve model and soils with measured soil water retention curve cannot be fitted well by the VGM model or the VG-BCB model.

ACKNOWLEDGEMENTS

The authors thank the anonymous reviewers for their helpful comments. This research was supported by the National Natural Science Foundation of China (Grant No. 91747204), State Environmental Protection Key Laboratory of Integrated Surface Water-Groundwater Pollution Control, Strategic Priority Research Program of Chinese Academy of Sciences (Grant XDA20060402), High-level Special Funding of the Southern University of Science and Technology (Grant No. G02296302, G02296402), and an AXA Research Fund Post-Doctoral Fellowship awarded to X.K.

Data Availability Statement

All measured data were collected from the literature and all data have been cited in the bibliography.

Conflict of Interest Statement

The authors declare that there is no conflict of interest.

REFERENCES

Assouline, S. (2001). A model for soil relative hydraulic conductivity based on the water retention characteristic curve. *Water Resources Research*, *37*(2), 265–271.

Assouline, S. (2005). On the relationships between the pore size distribution index and characteristics of the soil hydraulic functions. *Water Resources Research*, *41*, W07019, doi:10.1029/2004WR003511.

Assouline, S., & Or, D. (2013). Conceptual and parametric representation of soil hydraulic properties: A review. *Vadose Zone Journal*, *12*(4), doi:10.2136/vzj2013.07.0121.

Assouline, S., & Selker, J. (2017). Introduction and evaluation of a Weibull hydraulic conductivity-pressure head relationship for unsaturated soils. *Water Resources Research*, *53*, 4956–4964.

Averjanov, S. F. (1950). About permeability of subsurface soils in case of incomplete saturation. *Engineering Collection*, *7*, 19–21.

Black, T. A., Gardner, W. R., & Thurtell, G. W. (1969). The prediction of evaporation, drainage, and soil water storage for a bare soil. *Soil Science Society of America Proceedings*, *33*(5), 655–660.

Bresler, E., Russo, D., & Miller, R. D. (1978). Rapid estimate of unsaturated hydraulic conductivity function. *Soil Science Society of America Journal*, *42*(1), 170–172.

Brooks, R. H. & Corey, A. T. (1964). Hydraulic Properties of Porous Media. *Hydrology Paper No 3*. Civil Engineering Department, Colorado State University, Fort Collins, CO.

Brutsaert, W. (1967). Some methods of calculating unsaturated permeability. *Transactions of the ASAE*, *10*(3), 400–404.

Brutsaert, W. (2000). A concise parameterization of the hydraulic conductivity of unsaturated soils. *Advances in Water Resources*, *23*, 811–815.

Burdine, N. T. (1953). Relative permeability calculations from pore size distribution data. *Transactions of the American Institute of Mining Engineers*, *198*, 71–78.

Chen, H., Chen, K., & Yang, M. (2020). A new hysteresis model of the water retention curve based on pore expansion and contraction. *Computers and Geotechnics*, *121*, 103482.

Childs, E. C., & Collis-George, N. (1950). The permeability of porous materials. *Proceedings of the Royal Society of London. Series A, Mathematical and Physical Sciences*, *201*(1066), 392–405.

Dury, O., Fischer, U., & Schulin, R. (1998). Dependence of hydraulic and pneumatic characteristics of soils on a dissolved organic compound. *Journal of Contaminant Hydrology*, *33*, 39–57.

Elrick, D. E., & Bowman, D. H. (1964). Note on an improved apparatus for soil moisture flow measurements. *Soil Science Society of America Proceedings*, *28*, 450–453.

Fatt, I. & Dykstra, H. (1951). Relative permeability studies. *Transactions of the American Institute of Mining Engineers*, *192*, 249–255.

Fuentes, C., Haverkamp, R., & Parlange, J.-Y. (1992). Parameter constraints on closed-form soilwater relationships. *Journal of Hydrology*, *134*, 117–142.

Green, R. E., Hanks, R. J., & Larson, W. E. (1964). Estimates of field infiltration by numerical solution of the moisture flow equation. *Soil Science Society of America Proceedings*, *28*(1), 15–19.

Haverkamp, R., Vauclin M., Touma, J., Wierenga, P. J. & Vachaud, G. (1977). A comparison of numerical simulation models for one-dimensional infiltration. *Soil Science Society of America Journal*, *41*(2), 285–294.

Haverkamp, R., Parlange, J. Y., Starr, J. L., Schmitz, G., & Fuentes, C. (1990). Infiltration under ponded conditions: 3. A predictive equation based on physical parameters. *Soil science, 149*(5), 292–300.

Hayek, M. (2016). Analytical solution to transient Richards' equation with realistic water profiles for vertical infiltration and parameter estimation. *Water Resources Research*, *52*, 4438–4457.

Hu, R., Chen, Y.-F., Liu, H.-H., & Zhou, C.-B. (2013). A water retention curve and unsaturated hydraulic conductivity model for deformable soils: consideration of the change in pore-size distribution. *Géotechnique*, *63*(16), 1389–1405.

Huang, S., Barbour, S. L., & Fredlund, D. G. (1998). Development and verification of a coefficient of permeability function for a deformable unsaturated soil. *Canadian Geotechnical Journal*, *35*(3), 411–425.

Iden, S. C., Peters, A., & Durner, W. (2015). Improving prediction of hydraulic conductivity by constraining capillary bundle models to a maximum pore size. *Advances in Water Resources*, *85*, 86–92.

Ippisch, O., Vogel, H.-J., & Bastian, P. (2006). Validity limits for the van Genuchten-Mualem model and implications for parameter estimation and numerical simulation. *Advances in Water Resources*, *29*, 1780–1789.

Irmay, S. (1954). On the hydraulic conductivity of unsaturated soils. *Transactions American Geophysical Union*, *35*(3), 463–467.

Jensen, M. E., & Hanks, R. J. (1967). Nonsteady-state drainage from porous media. *Journal of the Irrigation and Drainage Division*, *93*(IR3), 209–231.

Jackson, R. D., Reginato, R. J., & van Bavel, C. H. M. (1965). Comparison of measured and calculated hydraulic conductivities of unsaturated soils. *Water Resources Research*, *1*(3), 375–380.

Kamai, T., & Assouline, S. (2018). Evaporation from deep aquifers in arid regions: Analytical model for combined liquid and vapor water fluxes. *Water Resources Research*, *54*, 4805–4822.

Kastanek, F. (1971). Numerical simulation technique for vertical drainage from a soil column. *Journal of Hydrology*, *14*, 213–232.

Kong, J., Shen, C., Luo, Z., Hua, G., & Zhao, H. (2016). Improvement of the hillslope-storage Boussinesq model by considering lateral flow in the unsaturated zone. *Water Resources Research*, *52*(4), 2965–2984.

Kosugi, K. (1999). General model for unsaturated hydraulic conductivity for soils with lognormal pore-size distribution. *Soil Science Society of America Journal*, *63*(2), 270–277.

Kuang, X., & Jiao, J. J. (2014). A new equation for the soil water retention curve. *European Journal of Soil Science*, *65*(4), 584–593.

Kuang, X., Jiao, J. J., Wan, L., Wang, X., & Mao, D. (2011). Air and water flows in a vertical sand column. *Water Resources Research*, *47*(4), W04506, doi:10.1029/2009WR009030.

Leij, F. J., Alves, W. J., van Genuchten, M. T., & Williams, J. R. (1996). *The UNSODA Unsaturated Soil Hydraulic Database, User's Manual Version 1.0*, EPA/600/R-96/095, National Risk Management Research Laboratory. Office of Research and Development. U.S. Environmental Protection Agency, Cincinnati, OH.

Luckner, L., van Genuchten, M. T., & Nielsen, D. R. (1989). A consistent set of parametric models for the two-phase flow of immiscible fluids in the subsurface. *Water Resources Research*, *25*(10), 2187–2193.

Luo, Z., Kong, J., Shen, C., Lu, C., Hua, G., Zhao, Z., Zhao, H., & Li, L. (2019). Evaluation and application of the modified van Genuchten function for unsaturated porous media. *Journal of Hydrology*, *571*, 279–287.

Madi, R., de Rooij, G. H., Mielenz, H., & Mai, J. (2018). Parametric soil water retention models: a critical evaluation of expressions for the full moisture range. *Hydrology and Earth System Sciences*, *22*, 1193–1219.

Marquardt, D.W. (1963). An algorithm for least-squares estimation of nonlinear parameters. *Journal of the Society for Industrial & Applied Mathematics*, *11*, 431–441.

Mendenhall, W., & Sincich, T. (2012). *A Second Course in Statistics: Regression Analysis*, 7th ed., Prentice Hall, Boston.

Mualem, Y. (1974). *A catalogue of the hydraulic properties of unsaturated soils*. Haifa, Israel: Technion Israel Institute of Technology, Technion Research & Development Foundation.

Mualem, Y. (1976). A new model for predicting the hydraulic conductivity of unsaturated porous media. *Water Resources Research*, *12*(3), 513–522.

Mualem, Y. (1978). Hydraulic conductivity of unsaturated porous media: Generalized macroscopic approach. *Water Resources Research*, *14*(2), 325–334.

Mualem, Y., & Dagan, G. (1978). Hydraulic conductivity of soils: Unified approach to the statistical models. *Soil Science Society of America Journal*, *42*(3), 392–395.

Nemes, A., Schaap, M. G., & Leij, F. J. (1999). *The UNSODA Unsaturated Soil Hydraulic Database*, *Version 2.0*, U. S. Salinity Laboratory, Riverside, California.

Nemes, A., Schaap, M. G., Leij, F. J., & Wösten, J. H. M. (2001). Description of the unsaturated soil hydraulic database UNSODA version 2.0. *Journal of Hydrology*, *251*, 151–162.

Parlange, J. Y., Haverkamp, R., & Touma, J. (1985). Infiltration under ponded conditions: 1. Optimal analytical solution and comparison with experimental observations. *Soil Science*, *139*(4), 305–311.

Philip, J. R. (1957). The theory of infiltration: 1. The infiltration equation and its solution, *Soil Science*, *83*(5), 345–357.

Poulovassilis, A. (1970a). Hysteresis of pore water in granular porous bodies. *Soil Science*, *109*(1), 5–12.

Poulovassilis, A. (1970b). The effect of the entrapped air on the hysteresis curves of a porous body and on its hydraulic conductivity. *Soil Science*, *109*(3), 154–162.

Press, W. H., Teukolsky, S. A., Vetterling, W. T. & Flannery, B. P. (1992). *Numerical Recipes in Fortran 77: The Art of Scientific Computing*, 2nd edition. Cambridge University Press, Cambridge.

Romero, E., Della Vecchia G., Jommi, C. (2011). An insight into the water retention properties of compacted clayey soils. *Géotechnique*, *61*(4), 313–328.

Schaap, M. G., & Leij, F. J. (2000). Improved prediction of unsaturated hydraulic conductivity with the Mualem-van Genuchten model. *Soil Science Society of America Journal*, *64*, 843–851.

Schaap, M. G., & van Genuchten, M. T. (2006). A modified Mualem-van Genuchten formulation for improved description of the hydraulic conductivity near saturation. *Vadose Zone Journal*, *5*, 27–34.

Staple, W. J. (1965). Moisture tension, diffusivity, and conductivity of a loam soil during wetting and drying, *Canadian Journal of Soil Science*, *45*, 78–86.

Tao, G., Zhu, X., Cai, J., Xiao, H., Chen, Q., & Chen, Y. (2019). A fractal approach for predicting unsaturated hydraulic conductivity of deformable clay. *Geofluids*, *2019*, 8013851.

Topp, G. C. (1971). Soil water hysteresis in silt loam and clay loam soils. *Water Resources Research*, *7*(4), 914–920.

Touma, J. (2009). Comparison of the soil hydraulic conductivity predicted from its water retention expressed by the equation of Van Genuchten and different capillary models, *European Journal of Soil Science*, *60*(4), 671–680.

Touma, J., & Vauclin, M. (1986), Experimental and numerical analysis of two-phase infiltration in a partially saturated soil. *Transport in Porous Media*, *1*, 27–55.

Troch, P. (1993). Conceptual basin-scale runoff process models for humid catchments: Analysis, synthesis and applications. PhD Dissertation, 247pp., Faculty of Agricultural and Applied Biological Sciences, Ghent University, Ghent, Belgium.

Tuli, A., & Hopmans, J. W. (2004). Effect of degree of fluid saturation on transport coefficients in disturbed soils. *European Journal of Soil Science*, *55*, 147–164.

van Genuchten, M. T. (1980). A closed-form equation for predicting the hydraulic conductivity of unsaturated soils. *Soil Science Society of America Journal*, *44*(5), 892–898.

van Genuchten, M. T., & Nielsen, D. R. (1985). On describing and predicting the hydraulic properties of unsaturated soils. *Annales Geophysicae*, *3*(5), 615–628.

Vogel, T., & Cislerova, M. (1988). On the reliability of unsaturated hydraulic conductivity calculated from the moisture retention curve. *Transport in Porous Media*, *3*, 1–15.

Vogel, T., van Genuchten, M. T., & Cislerova, M. (2001). Effect of the shape of the soil hydraulic functions near saturation on variably-saturated flow predictions. *Advances in Water Resources*, *24*, 133–144.

Watson, K. K. (1967). Experimental and numerical study of column drainage. *Journal of the Hydraulics Division*, *93*(2), 1–15.

Yuster, S. T. (1951). Theoretical considerations of multiphase flow in idealized capillary systems. *Proceedings Third World Petroleum Congress-Section II*, 437–445.

TABLE 1 Soil properties for the selected 59 soils

Soil no.	Soil name	K_s (cm/d)	θ_s	Reference
1	Hygiene sandstone	16.8	0.250	Brooks & Corey (1964)
2	Berea sandstone	45.4	0.206	Brooks & Corey (1964)
3	Botany sand fraction	1607.0	0.350	Watson (1967)
4	Glass beads	991.6	0.370	Brooks & Corey (1964)
5	Sand (0.25-0.5 mm)	–	0.364	Childs & Collis-George (1950)
6	Sand (0.5-1.0 mm)	–	0.357	Childs & Collis-George (1950)
7	Sand fraction (150-300 um)	1030.7	0.372	Kastanek (1971)
8	Sable de Riviere	–	0.342	Assouline & Or (2013)
9	Fragmented mixture	1416.5	0.443	Brooks & Corey (1964)
10	Fine sand (G. E. -13)	108.0	0.360	Jensen & Hanks (1967)
11	Sand (4443)	518.4	0.300	UNSODA
12	Volcanic sand	1038.8	0.351	Brooks & Corey (1964)
13	Fine sand (G. E. #13)	269.1	0.377	Brooks & Corey (1964)
14	Poudre river sand	2134.2	0.364	Brooks & Corey (1964)
15	Volcanic sand	700.0	0.350	Jensen & Hanks (1967)
16	Oso Flaco fine sand	1.1	0.406	Tuli & Hopmans (2004)
17	Sand	2178.5	0.304	Poulovassilis (1970b)
18	Mixed sand	969.9	0.285	Dury et al. (1998)
19	Sand (4445)	260.0	0.290	UNSODA
20	Sand	816.0	0.287	Haverkamp et al. (1977)
21	Plainfiled sand (25-60 cm depth)	266.0	0.304	Black et al. (1969)
22	Sand I_drying	1445.6	0.272	Poulovassilis (1970a)
23	Loamy sand (1010)	45.6	0.290	UNSODA
24	Sand I_wetting	1445.6	0.272	Poulovassilis (1970a)
25	Grenoble sand	369.6	0.312	Touma & Vauclin (1986)

26	Rehovot sand	657.5	0.400	Mualem (1974), Kamai & Assouline (2018)
27	Sand (1465)	40.0	0.320	UNSODA
28	Loamy sand (4062)	13.0	0.320	UNSODA
29	Sandy loam (3050)	19.5	0.499	UNSODA
30	Sandy loam (2241)	68.6	0.496	UNSODA
31	Sandy loam (2242)	209.0	0.544	UNSODA
32	Sandy loam (2243)	135.4	0.518	UNSODA
33	Sandy loam (1120)	37.9	0.293	UNSODA
34	Columbia sandy loam	1.9	0.427	Tuli & Hopmans (2004)
35	Gilat sandy loam	657.5	0.440	Mualem (1974), Kamai & Assouline (2018)
36	Wijgmaal sandy loam	8.2	0.397	Kosugi (1999)
37	Sandy clay loam (4791)	0.14	0.452	UNSODA
38	Sandy clay loam (4611)	0.055	0.452	UNSODA
39	Loam (4790)	36.3	0.504	UNSODA
40	Pachappa loam	13.1	0.456	Jackson et al. (1965)
41	Guelph loam	31.6	0.520	Elrick & Bowman (1964)
42	Loam (2530)	12.9	0.426	UNSODA
43	Touchet silt loam (G. E. #3)	47.2	0.485	Brooks & Corey (1964)
44	Touchet silt loam	21.7	0.480	Jensen & Hanks (1967)
45	Silt loam (2230)	21.7	0.430	UNSODA
46	Silt loam (2232)	27.8	0.463	UNSODA
47	Caribou silt loam	16.5	0.446	Topp (1971)
48	Silt loam (2231)	58.8	0.493	UNSODA
49	Ida silt loam (15-22.5 cm depth)	24.0	0.530	Green et al. (1964)
50	Grenville silt loam_wetting	28.3	0.475	Staple (1965)
51	Grenville silt loam_drying	28.3	0.475	Staple (1965)
52	Silt loam (4031)	5.4	0.443	UNSODA
53	Silt loam (2493)	45.5	0.452	UNSODA
54	Silt loam (4672)	2.4	0.394	UNSODA
55	Weld silty clay loam	49.0	0.470	Jensen & Hanks (1967)
56	Amarillo silty clay loam	221.0	0.455	Brooks & Corey (1964)
57	Silty clay (1360)	1.7	0.449	UNSODA
58	Yolo light clay	1.1	0.495	Philip (1957), Haverkamp et al. (1977)
59	Clay (2622)	0.57	0.445	UNSODA

TABLE 2 Fitted parameters for the van Genuchten (1980) function with different constraints on m and n

Soil no.	van Genuchten Equation 1 (m=1-1/n)			van Genuchten Equation 1 (m=1-2/n)			van Genuchten Equation 1 (n>2, 0<m<1)			
	θ_r	α (cm^{-1})	n	θ_r	α (cm^{-1})	n	θ_r	α (cm^{-1})	n	m
1	0.154	0.0159	10.64	0.153	0.0161	10.93	0.141	0.0185	23.11	0.163
2	0.0676	0.0194	8.91	0.0672	0.0198	9.284	0.0614	0.0229	22.89	0.169
3	0.0685	0.0232	27.35	0.0681	0.0232	27.62	0.0441	0.0248	80.78	0.126
4	0.0471	0.0313	19.78	0.0467	0.0314	20.05	0.0379	0.0335	33.84	0.285
5	0.0455	0.0354	17.95	0.0451	0.0355	18.28	0.0400	0.0373	24.90	0.439
6	0.0402	0.0557	17.37	0.0399	0.0560	17.70	0.0359	0.0590	25.13	0.408
7	0.0566	0.0256	13.26	0.0560	0.0259	13.54	0.0411	0.0296	47.84	0.102
8	0.0860	0.0474	7.834	0.0853	0.0487	8.122	0.0785	0.0559	12.00	0.292
9	0.143	0.0465	7.591	0.141	0.0478	7.873	0.133	0.0525	9.605	0.423
10	0.0732	0.0208	7.425	0.0710	0.0214	7.774	0.0751	0.0203	7.149	0.997

11	0.0291	0.0438	7.193	0.0274	0.0451	7.579	0.0180	0.0505	10.94	0.342
12	0.0688	0.0462	7.04	0.0675	0.0478	7.28	0.0543	0.0601	15.72	0.153
13	0.0716	0.0208	6.912	0.0692	0.0215	7.262	0.0713	0.0209	6.952	0.838
14	0.0586	0.0606	6.71	0.0549	0.0627	7.03	0	0.0790	23.51	0.0862
15	0.0720	0.0469	6.154	0.0700	0.0489	6.528	0.0540	0.0594	14.65	0.168
16	0.0690	0.0187	6.084	0.0675	0.0195	6.495	0.0705	0.0179	5.768	1.000
17	0	0.0330	5.813	0	0.0346	6.205	0	0.0354	6.424	0.617
18	0.0238	0.0312	5.773	0.0216	0.0326	6.194	0.0190	0.0341	6.775	0.545
19	0.0488	0.0169	5.448	0.0411	0.0177	5.686	0	0.0212	7.813	0.240
20	0.0724	0.0303	4.113	0.0665	0.0333	4.498	0.0670	0.0330	4.462	0.570
21	0.0688	0.0312	4.026	0.0661	0.0344	4.522	0.0634	0.0370	5.142	0.427
22	0	0.0366	4.043	0	0.0395	4.879	0	0.0331	3.779	0.988
23	0.102	0.0218	3.853	0.0930	0.0242	4.195	0.100	0.0221	3.893	0.707
24	0.0667	0.0624	3.765	0.0549	0.0695	4.077	0.0740	0.0564	3.559	0.999
25	0.0254	0.0437	2.238	6.38×10^{-6}	0.0585	2.839	0.0029	0.0524	2.463	0.375
26	0.0319	0.0570	2.087	0.0199	0.0778	2.811	0.0166	0.0832	3.142	0.242
27	0.0240	0.0210	1.800	0.0164	0.0301	2.614	0.0208	0.0247	2.001	0.354
28	5.53×10^{-7}	0.0277	1.374	2.80×10^{-10}	0.0382	2.339	1.23×10^{-6}	0.0356	2.000	0.174
29	0.292	0.0269	5.076	0.284	0.0284	5.328	0.088	0.0397	53.77	0.0125
30	0.155	0.0165	4.854	0.149	0.0177	5.246	0.125	0.0212	7.807	0.258
31	0.163	0.0239	4.842	0.157	0.0256	5.234	0.110	0.0327	11.51	0.141
32	0.156	0.0205	4.723	0.152	0.0220	5.140	0.114	0.0285	23.82	0.0659
33	0.0781	0.0133	1.836	0.0730	0.0187	2.663	0.0768	0.0148	2.002	0.387
34	0.0673	0.0125	1.573	0.0404	0.0193	2.414	0.0335	0.0207	2.808	0.138
35	4.50×10^{-7}	0.0113	1.468	2.40×10^{-7}	0.0181	2.380	6.00×10^{-7}	0.0157	2.000	0.203
36	0.0569	0.0153	1.392	0.0159	0.0266	2.261	0.0439	0.0214	2.000	0.163
37	0.136	0.0108	3.717	0.127	0.0121	4.133	0.114	0.0138	4.890	0.335
38	0.0820	0.0039	1.205	0	0.0076	2.129	0.0170	0.0072	2.000	0.0687
39	0.156	0.0140	3.638	0.147	0.0159	4.060	0.105	0.0213	7.870	0.142
40	0.0853	0.0068	2.314	0.0770	0.0089	3.002	0.0723	0.0098	3.580	0.251
41	0.204	0.0125	1.858	0.147	0.0198	2.474	0.132	0.0212	2.642	0.162
42	0.151	0.0183	1.504	0.128	0.0295	2.350	0.112	0.0359	5.316	0.0551
43	0.196	0.0101	6.945	0.193	0.0104	7.248	0.151	0.0129	15.20	0.147
44	0.187	0.0101	6.289	0.184	0.0105	6.644	0.138	0.0131	21.73	0.0929
45	0.134	0.0098	5.150	0.131	0.0104	5.550	0.100	0.0132	16.38	0.113
46	0.149	0.0116	4.700	0.144	0.0125	5.116	0.108	0.0162	20.15	0.0781
47	0.306	0.0076	4.148	0.302	0.0083	4.567	0.285	0.0107	10.65	0.131
48	0.145	0.0142	4.053	0.139	0.0157	4.492	0.0987	0.0211	14.48	0.0893
49	0.109	0.0125	1.579	0.0021	0.0217	2.307	0.0578	0.0181	2.000	0.199

50	0.0329	0.0278	1.309	0.0049	0.0467	2.232	0.0041	0.0472	2.274	0.101
51	0.0329	0.0109	1.240	0.0049	0.0163	2.196	0.0041	0.0177	4.574	0.0419
52	0.0031	0.0432	1.223	$1.44\text{x}10^{-7}$	0.0604	2.203	$1.30\text{x}10^{-5}$	0.0581	2.000	0.103
53	0.290	0.386	1.156	0.269	0.509	2.124	0.269	0.516	4.384	0.0281
54	0	0.0082	1.147	0	0.0134	2.129	0	0.0131	2.000	0.0648
55	0.163	0.0131	5.978	0.160	0.0137	6.349	0.115	0.0173	58.31	0.0325
56	0.128	0.0206	4.954	0.121	0.0219	5.316	0.134	0.0194	4.699	0.9998
57	0.0025	0.0045	1.110	0.001	0.0075	2.095	0.0005	0.0074	2.000	0.0477
58	0.162	0.0264	1.560	0.078	0.0471	2.296	0.056	0.0511	2.559	0.103
59	0.0014	0.0310	1.065	0	0.0492	2.059	0.0005	0.0486	2.000	0.0296

TABLE 3 The R^2 values for the VGM model, VG-BCB model, and the MVG-BCB model

Soil	$\theta(h)$			$K_r(\theta)$			$K_r(h)$		
no	VGM	VG-BCB	MVG-BCB	VGM	VG-BCB	MVG-BCB	VGM	VG-BCB	MVG-BCB
1	0.9944	0.9948	**0.9992**	0.9798	0.9813	**0.9844**	0.9450	0.9486	**0.9834**

2	0.9959	0.9964	**0.9996**	0.9854	0.9918	**0.9927**	0.9615	0.9713	**0.9931**
3	0.9905	0.9906	**0.9991**	**0.9985**	0.9859	0.9938			
4	0.9955	0.9957	**0.9980**				0.9713	0.9790	**0.9923**
5	0.9960	0.9961	**0.9968**	0.9675	0.9869	**0.9870**			
6	0.9976	0.9977	**0.9987**	**0.9831**	0.9644	0.9622			
7	0.9885	0.9891	**0.9993**				0.9767	**0.9830**	0.9764
8	0.9834	0.9846	**0.9922**	0.9902	0.9878	**0.9936**	0.9850	0.9892	**0.9917**
9	0.9972	0.9976	**0.9983**				0.8959	**0.9027**	0.9014
10	0.9984	0.9982	**0.9985**	0.8420	0.8591	**0.8604**			
11	0.9951	0.9956	**0.9967**	**0.9881**	0.9811	0.9807			
12	0.9944	0.9952	**0.9997**				0.9986	**0.9989**	0.9869
13	**0.9987**	0.9986	0.9987				0.8216	**0.8505**	0.8474
14	0.9952	0.9956	**0.9988**	0.9677	**0.9789**	0.9779	0.9235	0.9394	**0.9782**
15	0.9901	0.9919	**0.9997**	**0.9613**	0.9566	0.9503			
16	0.9808	0.9796	**0.9817**	0.9958	**0.9960**	0.9944			
17	0.9989	0.9991	**0.9992**	0.9816	**0.9843**	0.9829	0.9839	**0.9946**	0.9935
18	0.9966	0.9968	**0.9969**	0.9949	0.9987	**0.9988**			
19	0.9895	0.9903	**0.9925**	0.6285	0.7189	**0.7683**			
20	0.9978	**0.9979**	0.9979				**0.7417**	0.5317	0.5284
21	0.9982	0.9988	**0.9989**				0.9917	0.9960	**0.9973**
22	0.9970	0.9897	**0.9971**	0.9320	0.9740	**0.9822**			
23	**0.9892**	0.9891	0.9891	0.6993	0.8393	**0.8428**			
24	0.9983	0.9974	**0.9987**	0.8658	**0.9560**	0.9534			
25	0.9958	0.9956	**0.9959**	0.7802	**0.9549**	0.9459			
26	0.9925	0.9942	**0.9943**	0.3641	**0.7089**	0.6976			
27	0.9989	0.9981	**0.9990**	0.9024	**0.9960**	0.9918	0.6240	0.9419	**0.9703**
28	**0.9869**	0.9820	0.9833	0.5264	**0.7185**	0.7113			
29	0.9818	0.9824	**0.9926**	0.8103	0.8565	**0.9217**			
30	0.9972	0.9978	**0.9987**				0.9223	0.9546	**0.9558**
31	0.9958	0.9968	**0.9998**				0.9741	0.9878	**0.9969**
32	0.9927	0.9941	**0.9998**				0.8717	0.9099	**0.9746**
33	**0.9958**	0.9943	0.9955	0.2890	0.8055	**0.8438**			
34	0.9975	0.9983	**0.9983**	**0.9992**	0.9049	0.9128			
35	**0.9969**	0.9887	0.9919	0.3907	0.8624	**0.8773**			
36	**0.9913**	0.9840	0.9859	0.3410	**0.7662**	0.7575			
37	0.9987	0.9993	**0.9996**	0.9378	**0.9719**	0.9709	0.8838	0.9438	**0.9509**
38	0.9974	**0.9987**	0.9986	-0.5481	0.5884	**0.5966**			
39	0.9954	0.9971	**0.9999**	**0.8714**	0.7985	0.8131			
40	0.9977	0.9985	**0.9986**	0.7280	**0.9487**	0.9436			

41	0.9941	0.9953	**0.9953**	0.8695	0.9855	**0.9858**			
42	0.9811	0.9873	**0.9900**	**0.6923**	-1.6721	-1.0160			
43	0.9949	0.9956	**0.9992**				**0.9472**	0.9289	0.8962
44	0.9893	0.9907	**0.9994**	**0.8196**	0.7617	0.7552			
45	0.9924	0.9937	**0.9985**				0.8424	0.8986	**0.9453**
46	0.9935	0.9948	**0.9995**				0.7904	0.8574	**0.9180**
47	0.9914	0.9922	**0.9938**	**0.9208**	0.8938	0.8993			
48	0.9935	0.9951	**0.9995**				0.9453	0.9581	**0.9677**
49	**0.9988**	0.9974	0.9980	0.7288	**0.7511**	0.7112			
50	0.9977	**0.9990**	0.9990	0.0044	0.9543	**0.9549**			
51	0.9810	0.9891	**0.9915**	**0.8313**	0.7569	0.7634			
52	**0.9870**	0.9794	0.9806	0.1236	**0.7694**	0.7626			
53	0.9912	0.9918	**0.9919**	-0.4184	0.1051	**0.2015**			
54	**0.9958**	0.9896	0.9902	-0.4244	0.9017	**0.9025**	-0.4279	0.9917	**0.9920**
55	0.9819	0.9838	**0.9994**	0.9821	0.9811	**0.9823**			
56	**0.9939**	0.9868	0.9888	0.8395	0.9104	**0.9123**			
57	**0.9931**	0.9860	0.9866	0.7977	**0.8072**	0.8042			
58	0.9981	0.9995	**0.9996**	0.7380	0.9808	**0.9827**			
59	**0.9865**	0.9766	0.9770				-0.5495	-0.5035	**-0.4663**

Values in bold script represent the greatest R^2 value.

List of Figure Captions

FIGURE 1 Comparison of measured and calculated soil water retention curve $\theta(h)$ and relative hydraulic conductivity $K_r(\theta)$ for four soils.

FIGURE 2 Comparison of measured and calculated soil water retention curve $\theta(h)$ and relative hydraulic conductivity $K_r(h)$ for four soils.

FIGURE 3 Comparison of root-mean-square-error (RMSE) for soil water retention curve fitted by the van Genuchten (1980) model with different constraints on *m* and *n*.

FIGURE 4 Comparison of root-mean-square-error (RMSE) for different relative hydraulic conductivity models. (a) RMSE for relative hydraulic conductivity $K_r(\theta)$; (b) RMSE for relative hydraulic conductivity $K_r(h)$.

FIGURE 5 Measured and calculated soil water retention curve $\theta(h)$ and relative hydraulic conductivity $K_r(\theta)$ for Grenoble sand.

FIGURE 6 Comparison between simulated and measured cumulative infiltration data for (a) Grenoble sand and (b) Yolo light clay.

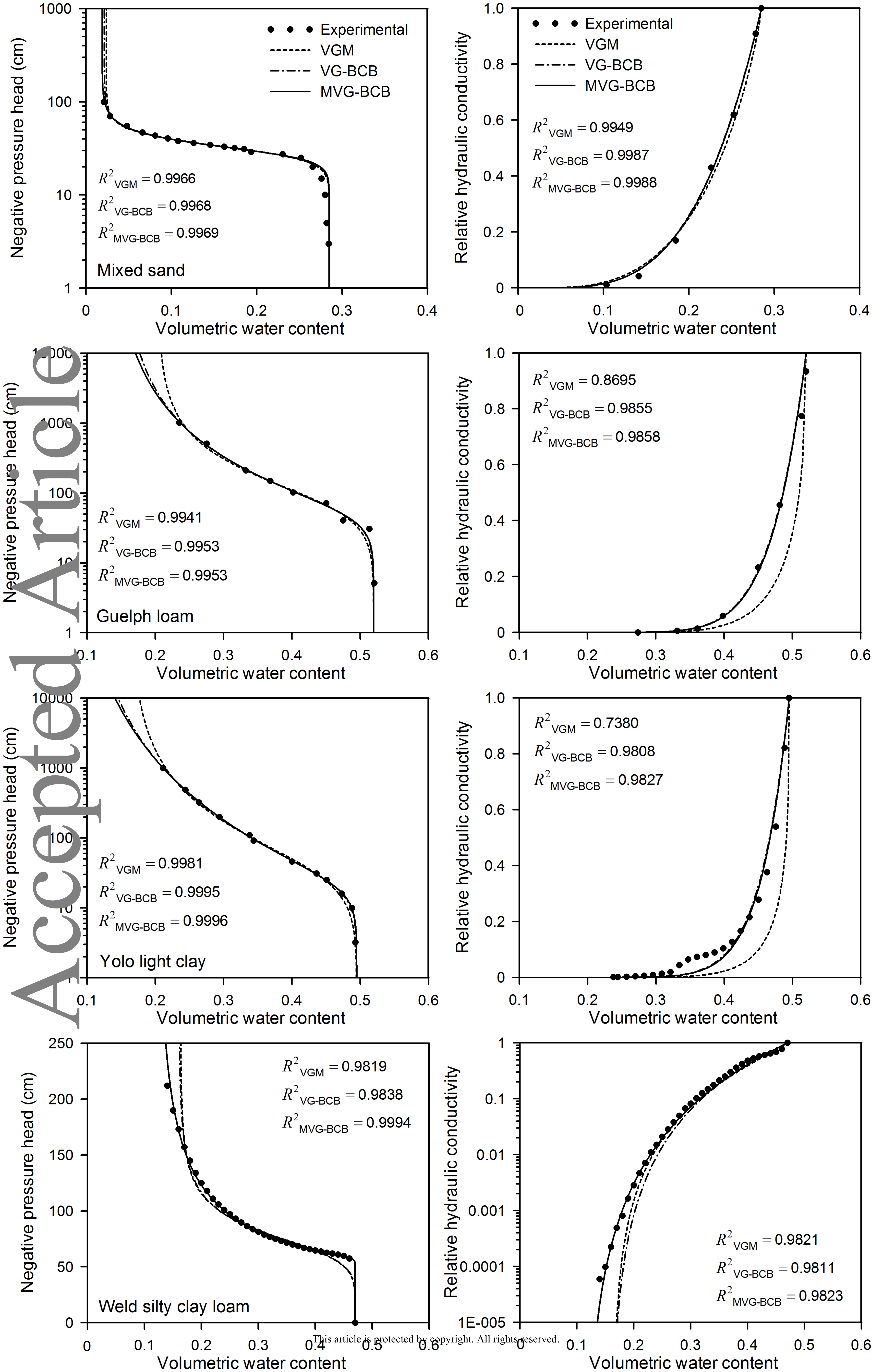

Experimental
VGM
VG-BCB
MVG-BCB
Negative pressure head (cm)
Volumetric water content
Relative hydraulic conductivity
$R^2_{VGM} = 0.9966$
$R^2_{VG\text{-}BCB} = 0.9968$
$R^2_{MVG\text{-}BCB} = 0.9969$
Mixed sand
$R^2_{VGM} = 0.9949$
$R^2_{VG\text{-}BCB} = 0.9987$
$R^2_{MVG\text{-}BCB} = 0.9988$
$R^2_{VGM} = 0.9941$
$R^2_{VG\text{-}BCB} = 0.9953$
$R^2_{MVG\text{-}BCB} = 0.9953$
Guelph loam
$R^2_{VGM} = 0.8695$
$R^2_{VG\text{-}BCB} = 0.9855$
$R^2_{MVG\text{-}BCB} = 0.9858$
$R^2_{VGM} = 0.9981$
$R^2_{VG\text{-}BCB} = 0.9995$
$R^2_{MVG\text{-}BCB} = 0.9996$
Yolo light clay
$R^2_{VGM} = 0.7380$
$R^2_{VG\text{-}BCB} = 0.9808$
$R^2_{MVG\text{-}BCB} = 0.9827$
$R^2_{VGM} = 0.9819$
$R^2_{VG\text{-}BCB} = 0.9838$
$R^2_{MVG\text{-}BCB} = 0.9994$
Weld silty clay loam
$R^2_{VGM} = 0.9821$
$R^2_{VG\text{-}BCB} = 0.9811$
$R^2_{MVG\text{-}BCB} = 0.9823$

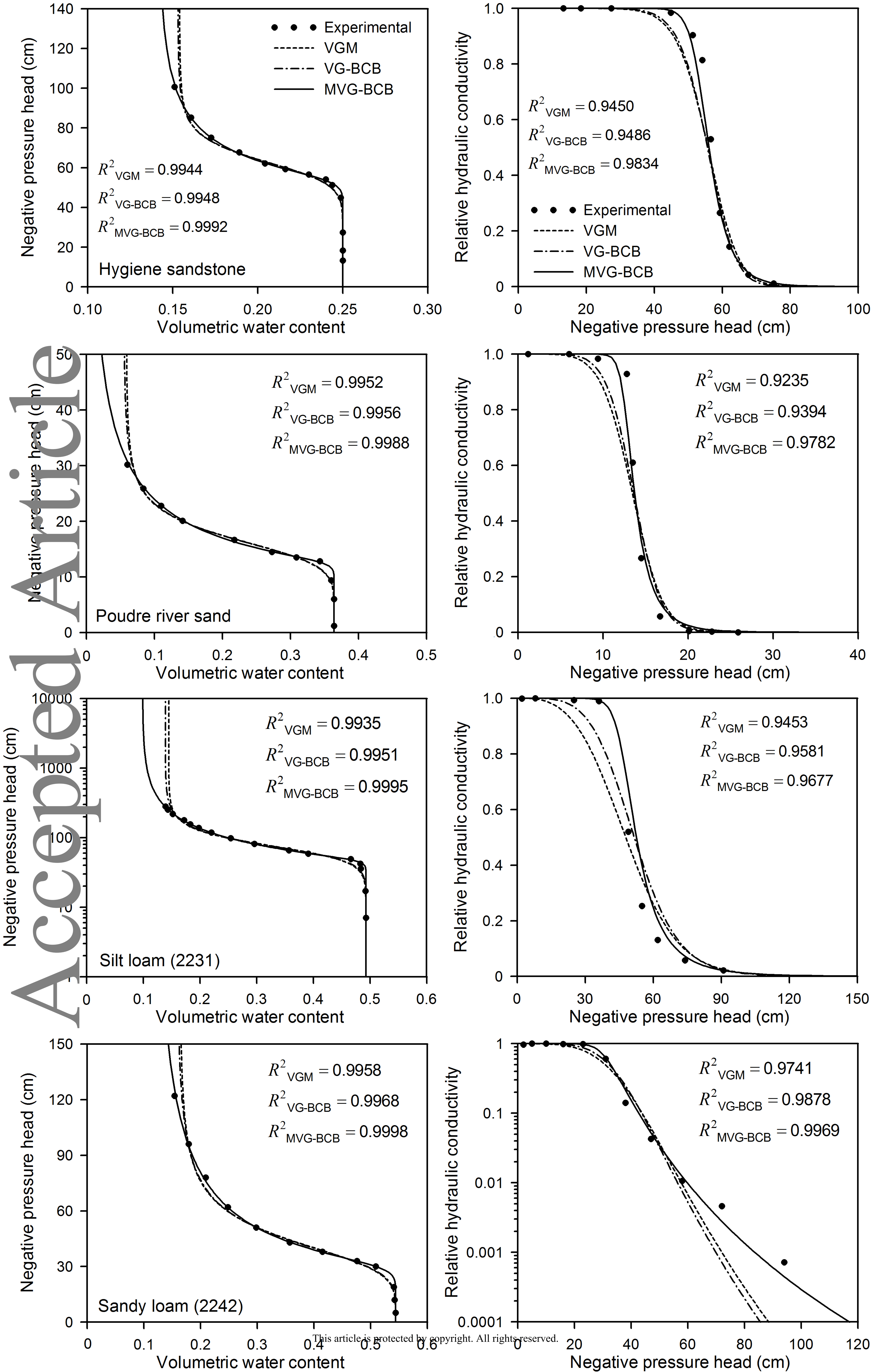
Experimental
VGM
VG-BCB
MVG-BCB
Negative pressure head (cm)
Volumetric water content
Relative hydraulic conductivity
Negative pressure head (cm)
Hygiene sandstone
$R^2_{VGM} = 0.9944$
$R^2_{VG\text{-}BCB} = 0.9948$
$R^2_{MVG\text{-}BCB} = 0.9992$
$R^2_{VGM} = 0.9450$
$R^2_{VG\text{-}BCB} = 0.9486$
$R^2_{MVG\text{-}BCB} = 0.9834$
Poudre river sand
$R^2_{VGM} = 0.9952$
$R^2_{VG\text{-}BCB} = 0.9956$
$R^2_{MVG\text{-}BCB} = 0.9988$
$R^2_{VGM} = 0.9235$
$R^2_{VG\text{-}BCB} = 0.9394$
$R^2_{MVG\text{-}BCB} = 0.9782$
Silt loam (2231)
$R^2_{VGM} = 0.9935$
$R^2_{VG\text{-}BCB} = 0.9951$
$R^2_{MVG\text{-}BCB} = 0.9995$
$R^2_{VGM} = 0.9453$
$R^2_{VG\text{-}BCB} = 0.9581$
$R^2_{MVG\text{-}BCB} = 0.9677$
Sandy loam (2242)
$R^2_{VGM} = 0.9958$
$R^2_{VG\text{-}BCB} = 0.9968$
$R^2_{MVG\text{-}BCB} = 0.9998$
$R^2_{VGM} = 0.9741$
$R^2_{VG\text{-}BCB} = 0.9878$
$R^2_{MVG\text{-}BCB} = 0.9969$

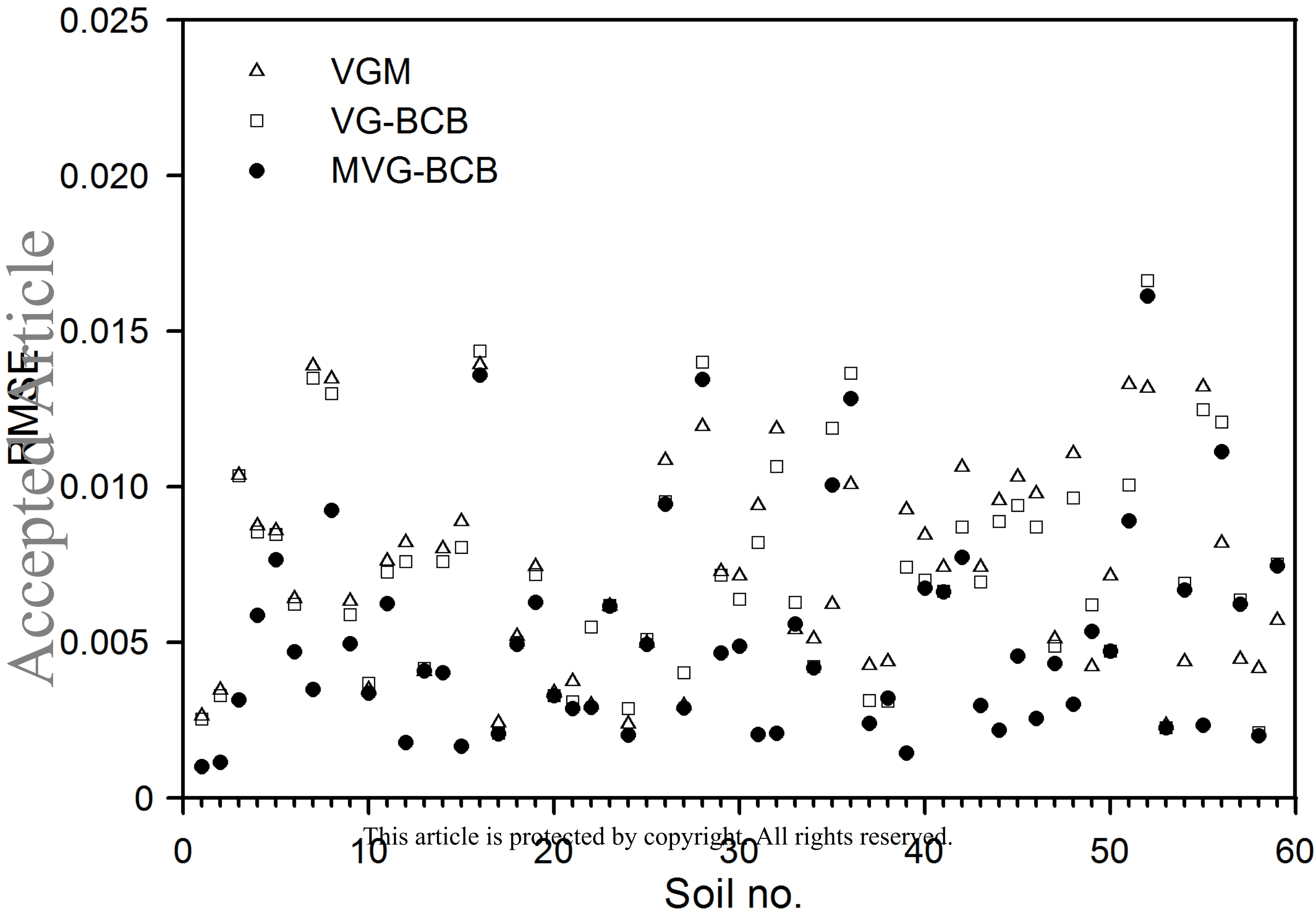

0.025
0.020
0.015
0.010
0.005
0
RMSE
VGM
VG-BCB
MVG-BCB
0
10
20
30
40
50
60
Soil no.

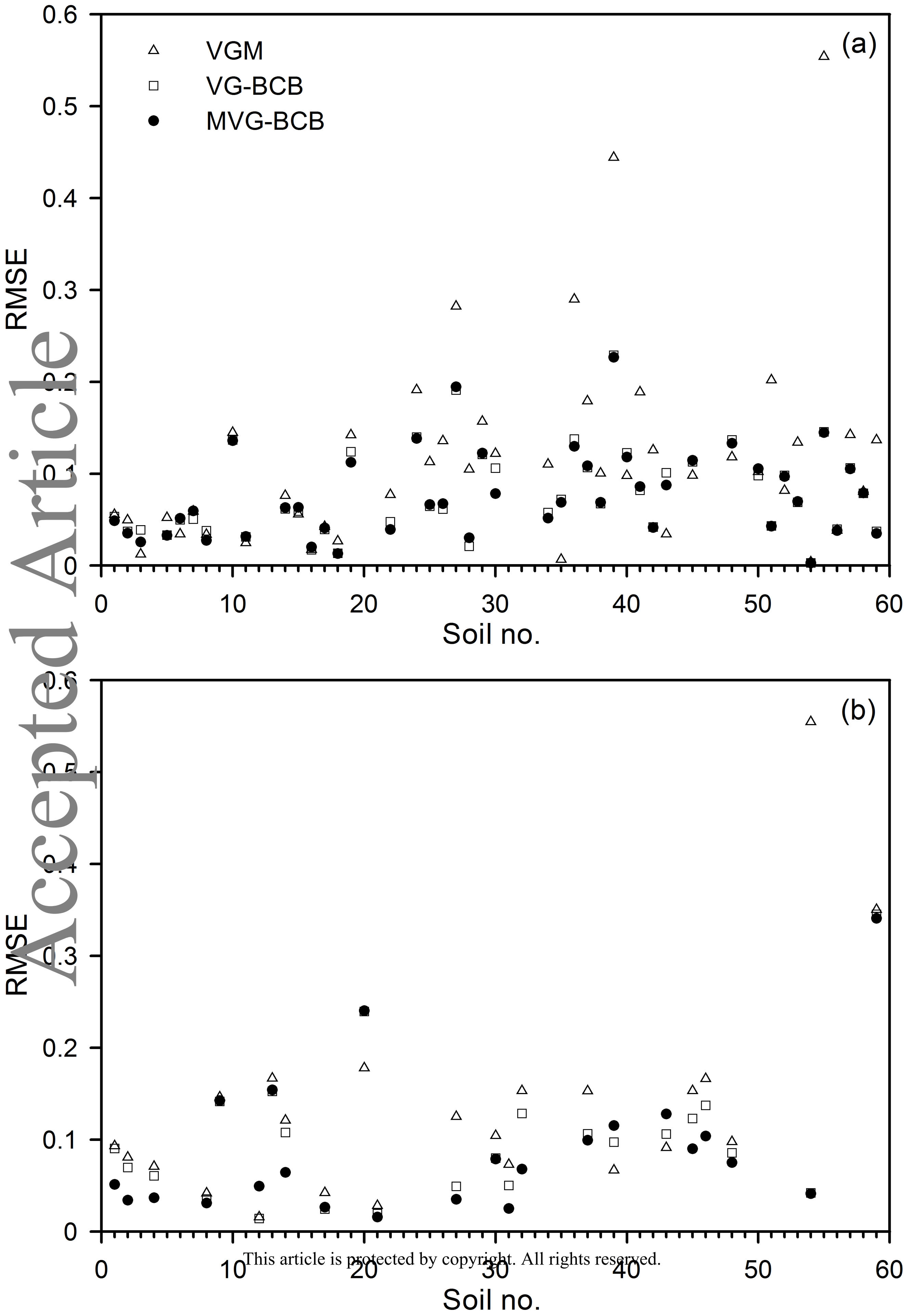

(a)
VGM
VG-BCB
MVG-BCB
RMSE
Soil no.
(b)
RMSE
Soil no.

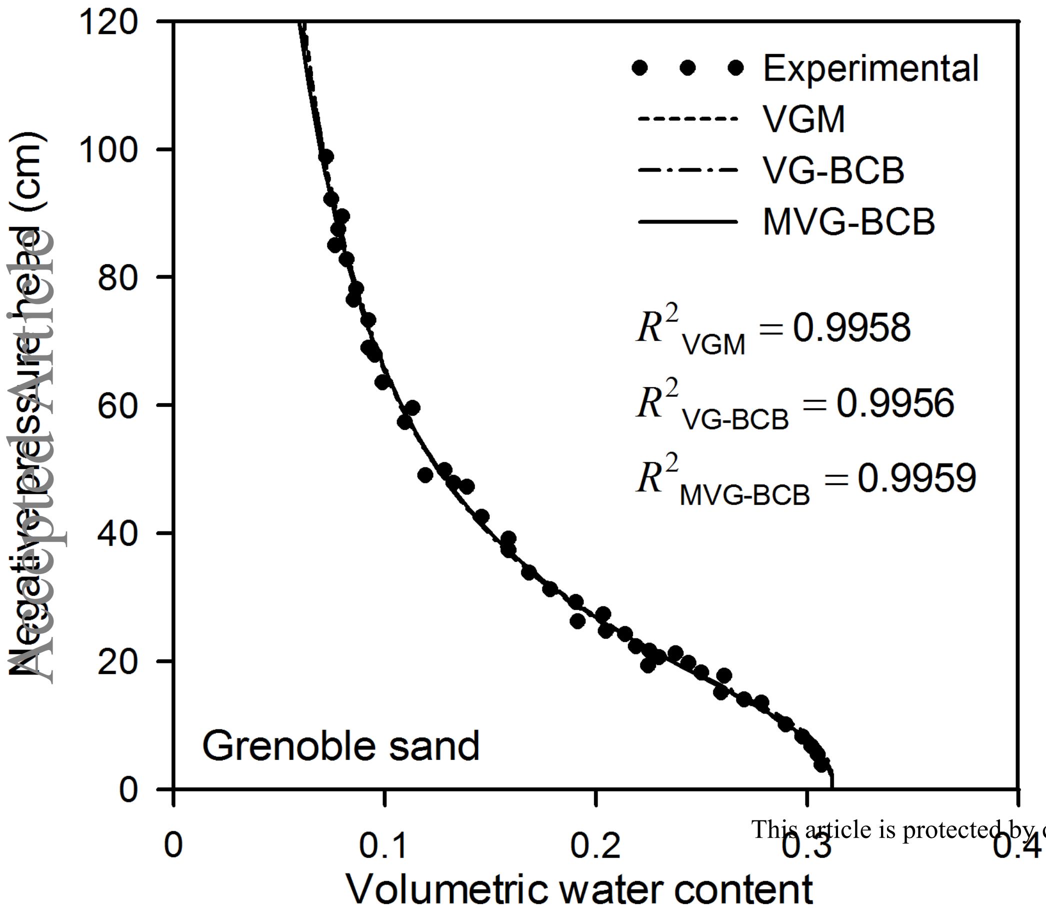

Negative pressure head (cm)
Volumetric water content
Experimental
VGM
VG-BCB
MVG-BCB
R^2_{VGM} = 0.9958
R^2_{VG-BCB} = 0.9956
$R^2_{MVG-BCB}$ = 0.9959
Grenoble sand

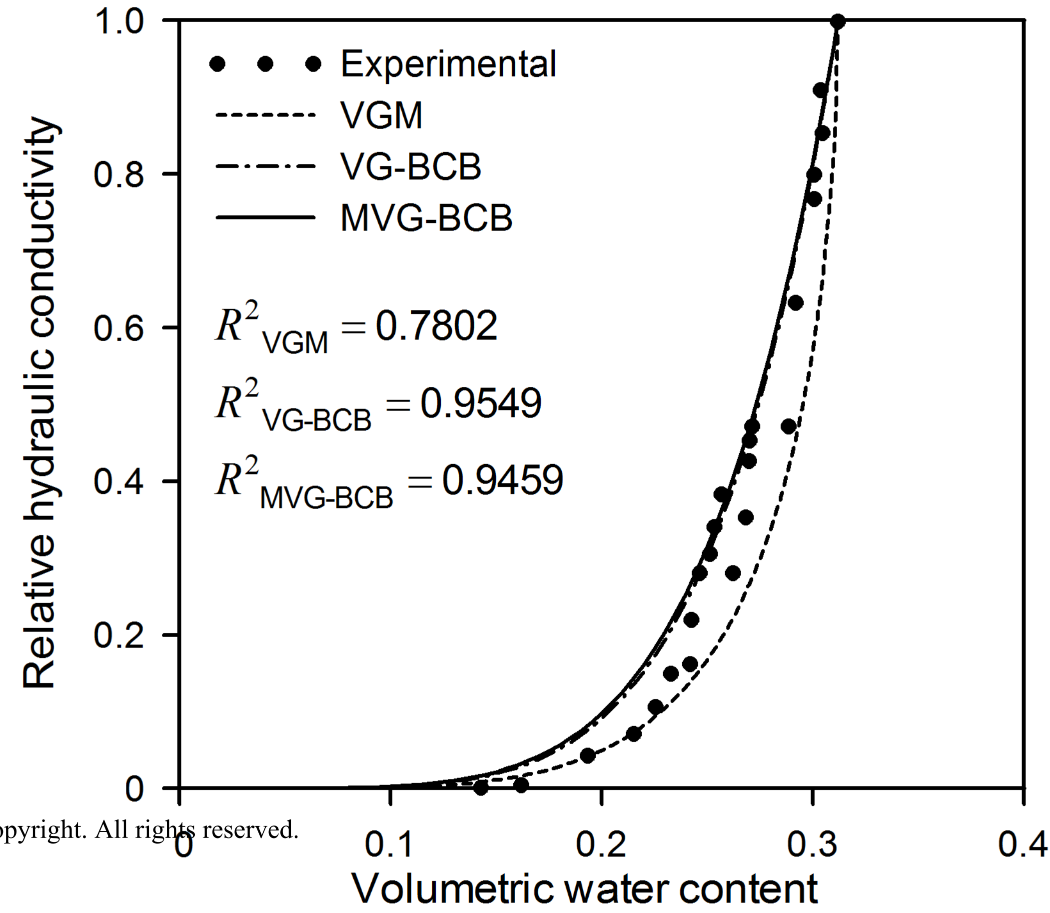

Relative hydraulic conductivity
Volumetric water content
Experimental
VGM
VG-BCB
MVG-BCB
R^2_{VGM} = 0.7802
R^2_{VG-BCB} = 0.9549
$R^2_{MVG-BCB}$ = 0.9459

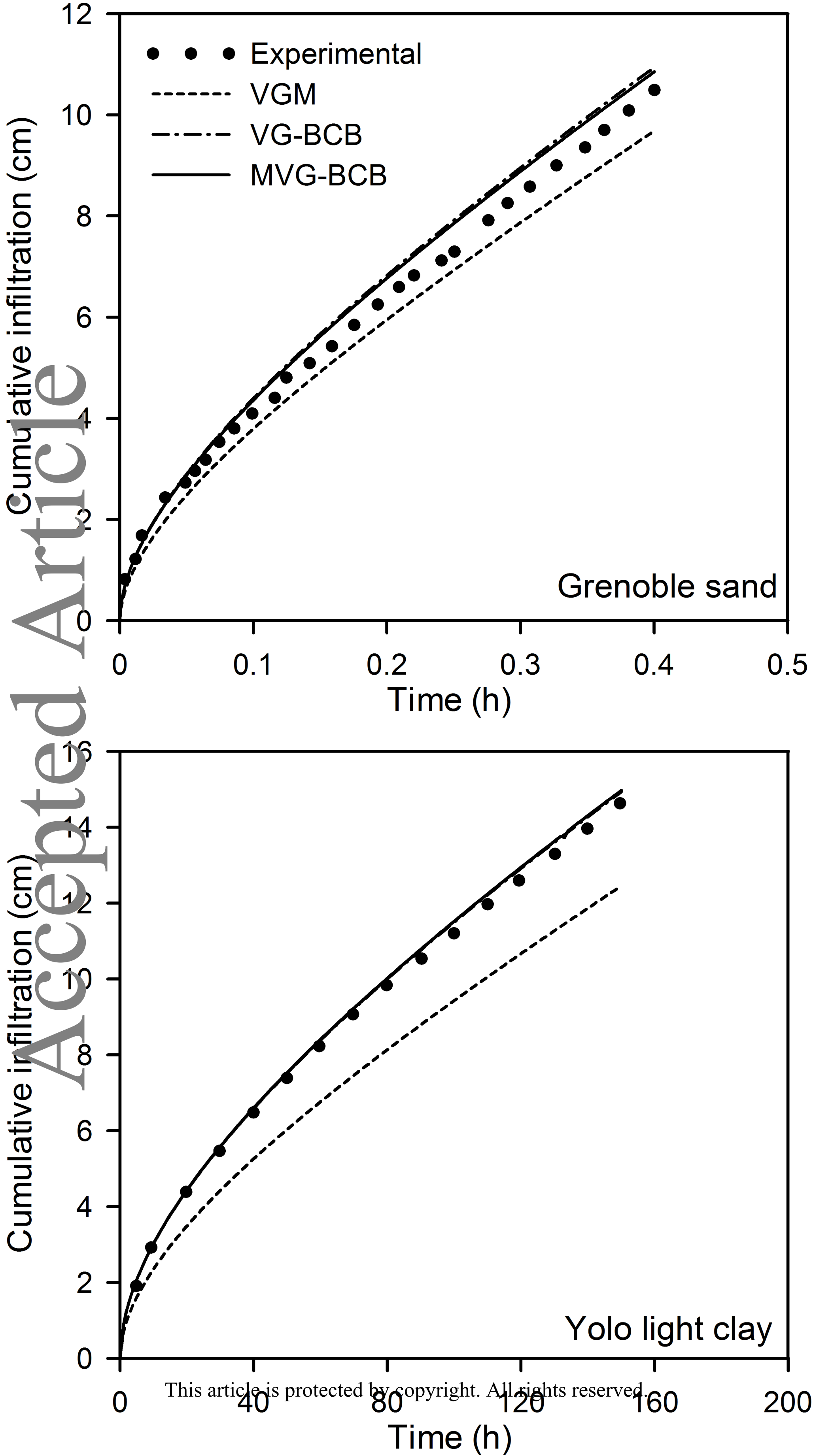

Experimental
VGM
VG-BCB
MVG-BCB
Cumulative infiltration (cm)
Time (h)
Grenoble sand
Yolo light clay